A COMPARISON OF STATNAMIC AND STATIC LOAD TESTS ON STEEL PIPE PILES IN THE FRASER DELTA

M. Janes[1], A. Sy[2] and R.G. Campanella[3]

ABSTRACT

Statnamic load testing was performed in October 1990 on individual piles at the University of British Columbia (UBC) pile research site near the North approach ramp to the Alex Fraser Bridge in Queensborough, Lulu Island, British Columbia. Site characterization and static pile load tests had been performed on the piles as part of the UBC research to develop correlations between in-situ tests and axial and lateral pile capacities. Additional testing carried out on the piles included high-strain dynamic testing during restrike using the pile driving analyzer. The Statnamic load test results are presented in this paper. A recently proposed method to estimate the static load-deflection behaviour of piles from Statnamic test data is applied to the UBC test piles, and the results are compared to static load test data. It is shown that the approach can provide reasonable estimates of pile stiffness and pile capacity in soft, highly viscoelastic soils provided that the ultimate dynamic pile capacity is exceeded during the Statnamic loading.

INTRODUCTION

The Statnamic load test method has become widely used as a tool to quickly and economically determine the load-deflection behaviour and ultimate static capacity of large diameter deep foundations. The system has been found to be accurate for piles in non cohesive and stiff cohesive soils where viscoelastic or damping effects are minimal. The interpretation of the results of tests performed in saturated fine-grained soils has proven to be more difficult. Recent advances in understanding the Statnamic load test have resulted in a simplified method of using the field measurements to derive an equivalent static load-deflection curve from the Statnamic test data (Middendorp et al. 1992; Middendorp, 1993).

This study examines the results and interpretation of Statnamic tests performed on three steel pipe piles driven into soft silty clays and fine sands at the UBC pile research site. The results of the Statnamic load tests are compared to the static load test data.

---

[1] M.C. Janes Engineering Services, Vancouver, B.C.
[2] Klohn-Crippen Consultants Ltd., Richmond, B.C.
[3] University of British Columbia, Vancouver, B.C.

SITE CHARACTERISTICS

The pile research site is located at the eastern tip of Lulu Island (Richmond) which is within the postglacial Fraser River delta. The Fraser sediments are of Holocene age, up to about 240 m thick, and overlie glacial deposits of the Late Wisconsin age or older. Figure 1 shows the soil profile and cone penetration test (CPT) data to a depth of 75 m at the test site. Beneath the surface 2 m thick sand fill layer is soft organic silty clay to about 15 m depth. The silty clay deposit is underlain by fine to medium grained sands to about 30 m depth, below which are deep deposits of normally consolidated clayey silts with sand layers. The CPT profile in Fig. 1 gives a clear picture of the stratigraphic detail at the test site, including the interlayering in the deltaic sediments. The mean groundwater table at the site is about 2.0 m below ground surface and varies with the tidal fluctuations in the adjacent Fraser River.

As part of the UBC pile research program, six 324 mm diameter steel pipe piles were driven at the site. The test pile embedment depths are illustrated in Fig. 2. Table 1 summarizes the pile dimensions and embedments.

Table 1. Summary of Test Pile Dimensions and Embedments

Pile No.*	Embedded Length (m)	Wall Thickness (mm)	Length/Diameter Ratio	Pile Toe Condition
1	14.3	9.5	44	close
2	13.7	9.5	42	close
3	16.8	9.5	52	close
4	23.2	9.5	72	open
5	31.1	11.5	96	close
7	28.7	11.5	88	close

* All pipe piles have 324 mm outside diameter

STATIC AXIAL LOAD TESTS

Static axial load tests were conducted on five of the 324 mm O.D. test piles. Pile 1 had a large diameter sleeve for the first 2 m to isolate it from the upper sand fill zone. The Quick Load Test (QML) method of axial loading was used, with the load applied in approximately 5% increments of the anticipated failure load for the test pile. A summary of the pile driving and testing schedule for the five load tested piles is presented in Table 2, together with the measured capacities as defined by the Davisson's failure criterion. Figure 3 presents the load-displacement results of the static axial pile load tests. Note that Pile 4 was not loaded to failure, and

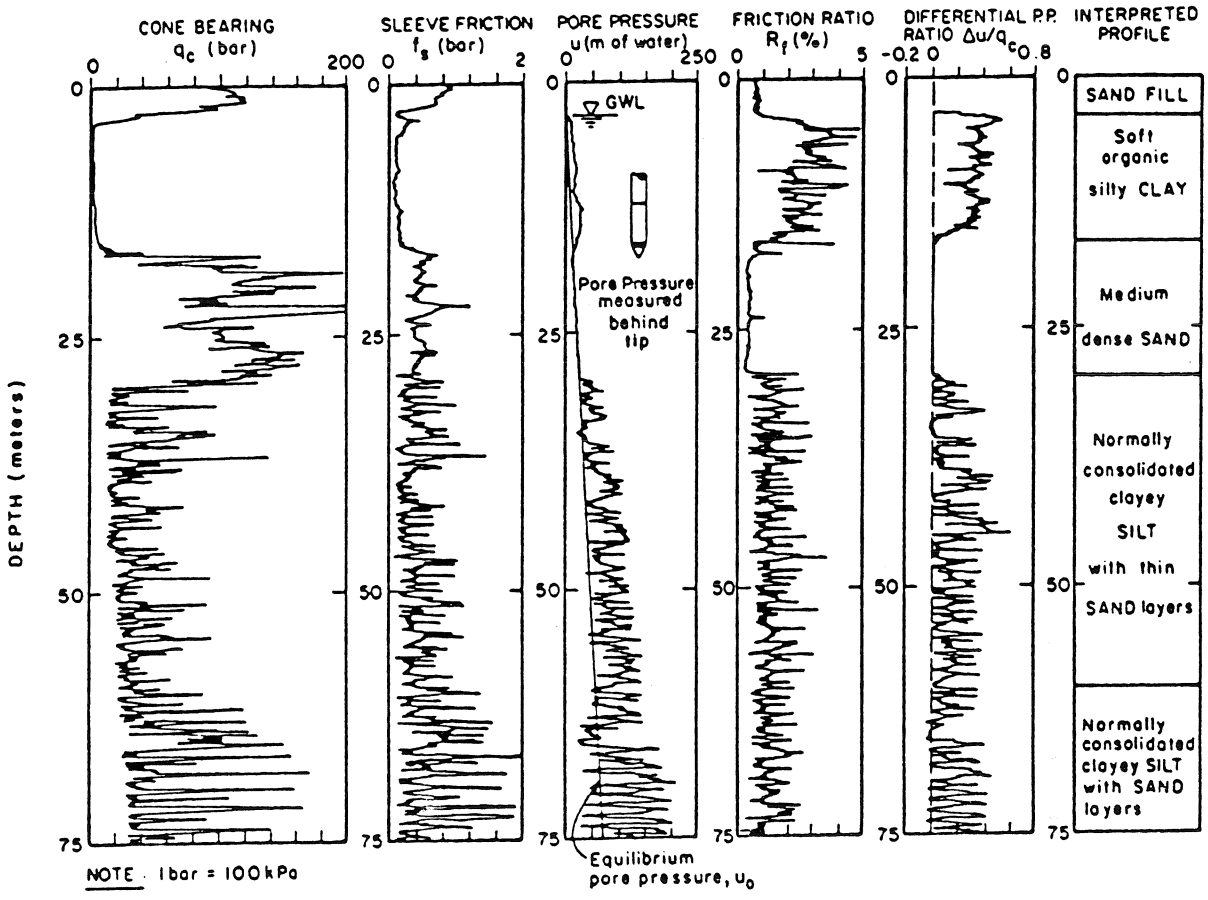

Fig. 1 CPT data at UBC pile research site, Lulu Island

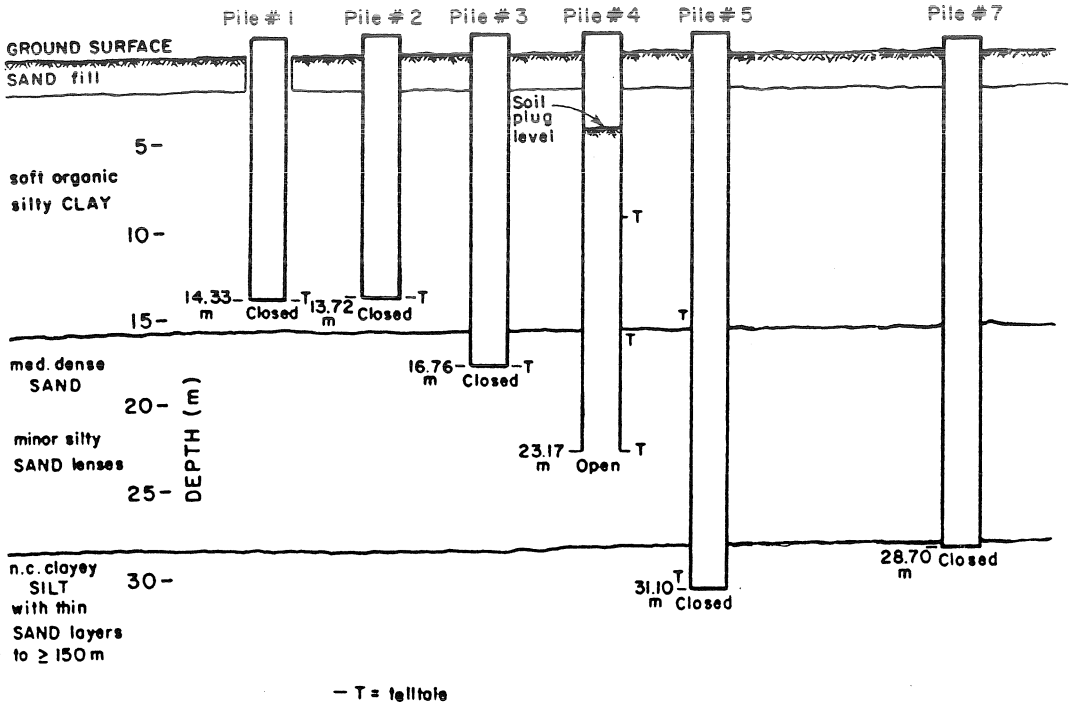

Fig. 2 Schematic of UBC test pile embedments

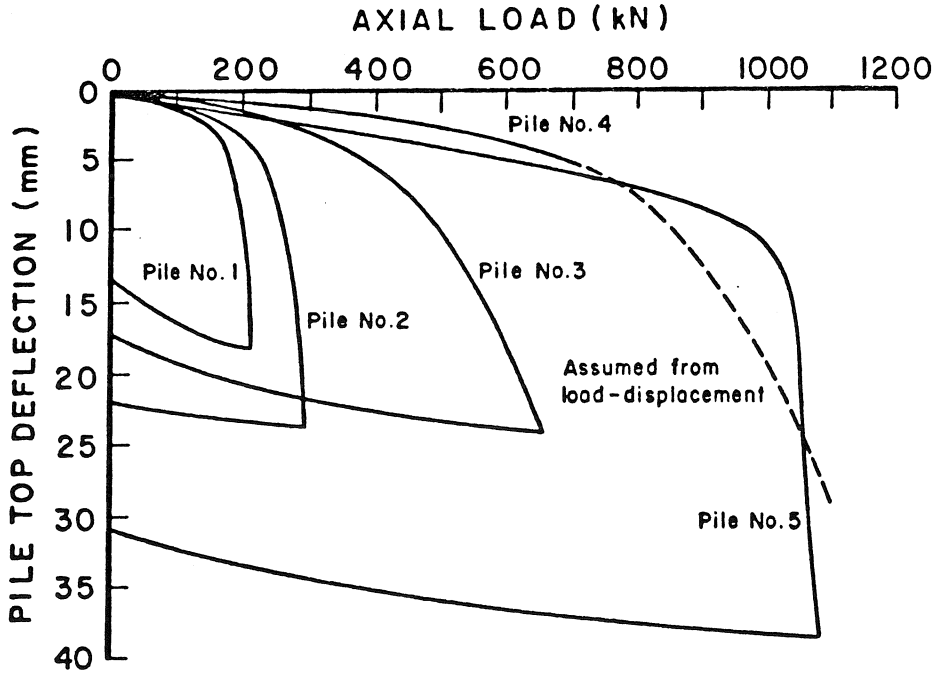

Fig. 3 Static axial pile load test results

consequently, the load-displacement curve beyond 700 kN was extrapolated based on the results of the other pile load tests (Robertson et al. 1988).

Table 2. Pile Driving and Static Load Testing Dates and Capacities

Pile No.	Driving Date	Testing Date	Capacity (kN)
1	Aug. 19, 1985	Nov. 9, 1985	170
2	Aug. 16, 1985	Mar. 1, 1986	220
3	Aug. 16, 1985	Nov. 9, 1985	610
4	Aug. 16, 1985	Mar. 1, 1986	1200
5	Aug. 15, 1985	Sep. 22, 1985	1070

DYNAMIC MEASUREMENTS DURING RESTRIKE

Piles 2, 3 and 5 were restruck in November 20, 1986. The piles were instrumented near the pile top with strain transducers and accelerometers during the restrike. The dynamic monitoring was conducted by Goble Rausche Likins and Associates of Seattle, Washington, USA, using the pile driving analyzer. The recorded force and integral of acceleration (velocity) data were used in the CAPWAP program (Rausche et al. 1985) to determine the static ultimate pile capacities. The CAPWAP analysis is a signal matching technique in which the measured pile signals are used, together with assumed boundary conditions, in a wave equation model to extract the best match pile capacity, resistance distribution with depth, and soil model parameters. Table 3 summarizes the CAPWAP computed capacities and measured capacities from the static load tests.

Table 3. Summary of CAPWAP and Static Pile Load Test Capacities

Pile No.	Restrike Blow No.	CAPWAP Capacity (kN)	Static Load Test Capacity (kN)
2	2	245	220
3	2	591	610
5	4	1139	1070

STATNAMIC LOAD TESTING

Statnamic Load Test Method

The Statnamic load test method uses the downward directed force generated through the launching of a reaction mass by quickly expanding gases within a pressure cylinder to load the top of a pile as shown schematically in Fig. 4. The gases are produced by the burning of a propellant fuel within the piston cylinder assembly. When the reaction mass assembly is accelerated upward at 20 g, a force acts equally downward on the pile foundation of the order of 20 times the reaction mass assembly. The duration of load, loading rate and the maximum load applied may be controlled with the piston and cylinder size, mass of the fuel, total reaction mass and venting of the gases. Loading of the pile is monitored using a calibrated load cell and displacement is monitored using a laser and photo voltaic cell. All data is recorded, digitized, stored and instantly displayed for the operator on a field computer (Bermingham and Janes, 1989).

The Statnamic load testing technique produces a dynamic load on the pile top which is slow enough to allow the pile to react as a rigid body without the influence of stress wave propagation within the pile. The soil in turn is loaded slowly enough to minimize inertial effects and damping. In highly viscoelastic soils, some rate effects are inevitable and influence the simplicity of interpreting the pile response. This study looks at the results of Statnamic load testing on piles installed in saturated fine-grained soils with high viscoelastic response.

Statnamic testing was performed at the UBC pile research site in October 1990. Prior to Statnamic testing, the piles had been retapped on July 30, 1990 in an effort to re-establish conditions somewhat similar to those at the time of the static load testing. Statnamic load testing was performed on Piles 3, 4, 5 and 7. Piles 1 and 2 were not tested as they did not have the capacity to withstand the minimum loading of the Statnamic device used in the study. Pile 7 is not discussed further as no comparative load test information is available on the pile.

Statnamic Load Test Interpretation

The procedure for the evaluation of Statnamic pile load-deflection response is based upon a simplified soil model and observations made of pile response to dynamic loading. The premise of the Statnamic loading period is such that stress wave propagation within the pile and soil are minimized and the system may be treated as a rigid body undergoing translation. Time dependent forces act upon the system and the system responds as a combination of pile and soil reactions. The pile reaction to loading is well understood as it represents a very stiff structural element with accurately known parameters describing its shape and material properties. The soil, however, is a non-engineered material with an undefined volume of influence. The analytical method, therefore, uses a combination of mathematically accurate dynamic equations with a simplified soil model, using information derived from observations at important points in the pile load-deflection response to calibrate the simplified soil model.

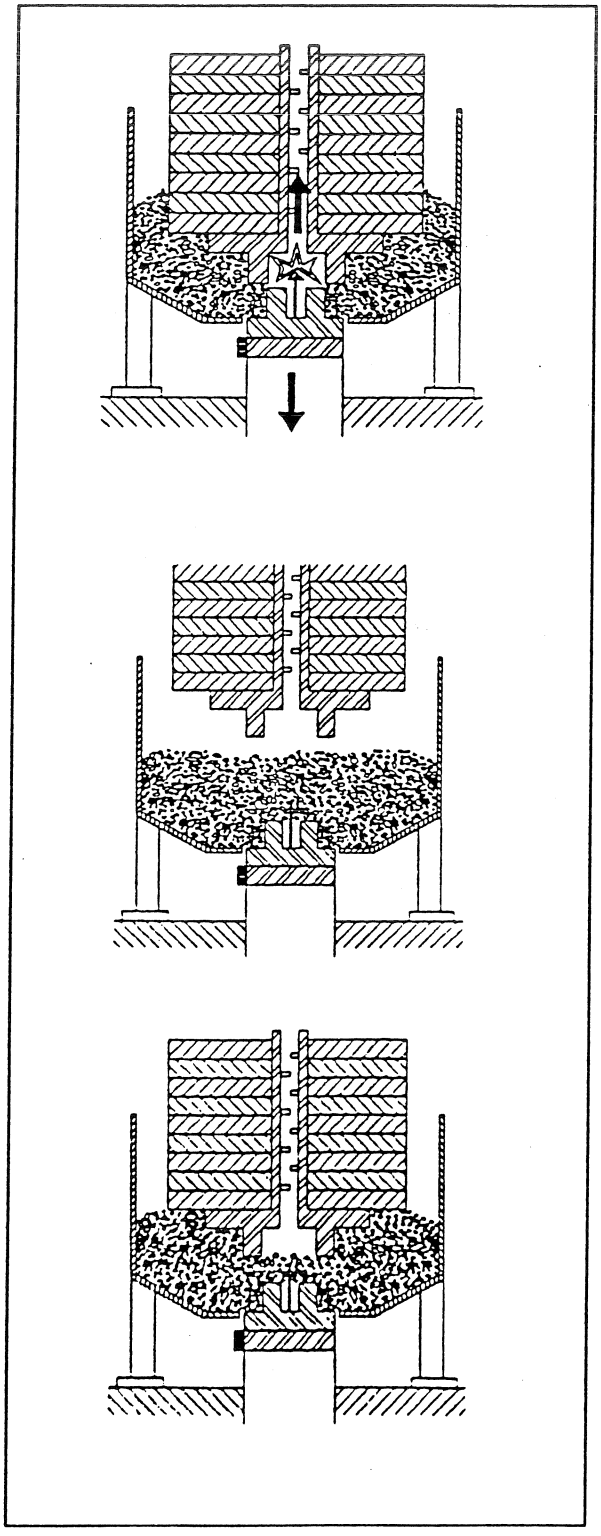

Fig. 4 Schematic of Statnamic load test

The response of a pile to a Statnamic loading event may be mathematically described as follows:

[1] $$F_{stn}(t) = F_u(t) + F_v(t) + F_a(t)$$

where:

$F_{stn}(t)$ is the term accounting for the Statnamic applied loading.

$F_u(t)$ is the term accounting for the static soil resistance. The effects upon soil resistance related to damping and acceleration are addressed in other terms. It should be noted that the Statnamic testing represents an undrained loading event of short duration. Thus viscoelastic effects due to increased porewater pressures are not accounted for.

$F_v(t)$ is the term accounting for the effect of damping upon the system. It is evaluated as the product of the damping coefficient (C) and the velocity of the pile. The pile velocity is obtained by differentiating the measured displacement of the top of the pile. The damping constant, C, represents a constant of proportionality between force and velocity and thus assumes only viscous damping.

$F_a(t)$ is the term accounting for the effect of inertia upon the system. It is evaluated as the product of acceleration of the pile and the mass of the pile. The mass of the pile is a known quantity and the acceleration is derived by twice differentiating the measured displacement of the top of the pile. It may be argued that some portion of the soil moves coincidentally with the pile prior to pile-soil interface failure and may be added to the pile mass for a more accurate evaluation of the inertial term.

Rewriting the equation to derive static capacity $F_u(t)$:

[2] $$F_u(t) = F_{stn}(t) - F_v(t) - F_a(t)$$

Equation [2] is useful as it may be solved for any time of loading (t) in order to construct a continuous pile load-deflection curve derived from the Statnamic event. In order to evaluate Eq. [2], the damping constant, C, must be established and it is assumed to remain the same throughout the test event. The damping effect can be derived through observation of the key events which occur in the Statnamic load-deflection curve. Figure 5 provides a typical Statnamic load-deflection curve for a pile undergoing significant net displacement. On the curve, five distinct events are observed as follows.

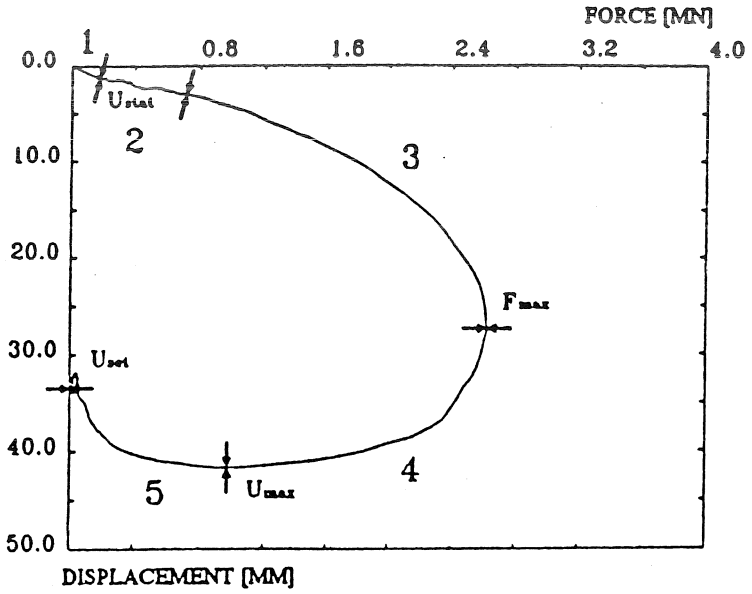

Fig. 5 Statnamic load-displacement curve characteristics

Section 1 represents the static load-deflection behaviour of the pile during the assembly of the Statnamic apparatus. As the piston and reaction masses are placed on the pile, load and deflection measurements are made which are used to construct this portion of the curve.

Section 2 represents the initial portion of the load-deflection curve produced during the Statnamic loading event. It provides the pile response due to a dynamic load prior to the onset of significant nonlinear soil behaviour. It follows closely along the same slope or stiffness of Section 1, the static portion of the curve. Pile and soil velocities and accelerations are very low through this section, which explains the similarity between the static and dynamic derived portions of the curve.

Section 3 represents the region where the onset of significant soil nonlinear behaviour influences the load-deflection curve through to the maximum loading exerted by the Statnamic test on the pile. In coincidence with the nonlinear soil behaviour, the pile and soil are mobilized to their highest level of downward velocity and acceleration. Thus the contributions of dynamic effects are at a maximum during this portion of the curve. In cases where the pile is sufficiently loaded to overcome the ultimate soil resistance, the full capacity of the pile is attained in this the section.

Section 4 represents the region of the curve from the beginning of load reduction through to the point of maximum pile top displacement. Note that maximum applied load and maximum pile top displacement do not coincide due to the downward momentum of the pile acquired during application of the Statnamic

load. The pile and soil during the loading have been mobilized and are travelling downward with some velocity. Upon unloading, the soil must overcome this momentum (momentum is the product of pile and soil mass times pile velocity) prior to reaching maximum displacement. The distance travelled by the pile under decreasing applied load is a rough measure of the dynamic nature and level of pile-soil failure of the Statnamic event. It is important to also note that the pile velocity at peak displacement is zero and thus the contribution of viscous damping is zero at that point.

Section 5 represents the coinciding rebound and unloading of the pile through to the final release of the pile from applied loading. If the full static capacity of the pile has been mobilized, some permanent displacement of the pile will result. It is important to note that the pile is now under the influence of loading upward from the soil and is mobilized by the soil at a rate compatible with the soil properties. Very little pile-soil interface slip or stress wave radiation occurs (hysteretic damping). Thus the rebound, though influenced somewhat by dynamic effect, is representative of true pile-soil linear behaviour.

Observations of the pile-soil behaviour at the end of Sections 3 and 4 prove to be very important to the evaluation of the Statnamic test results. The end of Section 4 coincides with the pile at zero velocity. Therefore, at this moment, the contribution of viscous damping to the system is zero. As a result, Eq. [2] describing pile-soil motion may now be simplified to:

[3] $$F_u(t_{umax}) = F_{stn}(t_{umax}) - F_a(t_{umax})$$

The static soil resistance and deflection (because we know the corresponding displacement at time t_{umax}) has now been established at one point, i.e at the point of maximum displacement. In order to calculate F_u at any time, which will reveal the corresponding displacement because we know the displacements at all times (t), we require knowledge of the damping constant, C. The damping constant may be established from the initial portion of the curve assuming the elastic pile-soil stiffness in Section 2 is the same as that of Section 1. However, the component magnitudes are small at these sections and are, therefore, subject to error.

Returning to Section 4, but this time directing attention to the point of maximum pile-soil resistance at the junction between Sections 3 and 4, we may make some observations. If the pile has been fully mobilized, then the resistance due to the soil will be a constant from peak loading at the beginning of Section 4 through to the maximum pile top displacement at the end of Section 4, and is equal to $F_u(t_{umax})$. In addition, if the sole contribution of damping is viscous, then a single damping coefficient, C_4, as calculated at the maximum applied loading occurring at the interface between Sections 3 and 4 would hold and we could rewrite Eq. [2] as:

[4] $$F_u(t_{umax}) = F_{stn}(t) - C_4 v(t) - ma(t)$$

Using the time dependent quantities at the maximum applied loading and rearranging Eq. [4], we may write an equation for C_4 as follows:

[5] $$C_4 = \frac{F_{stn}(t_4) - F_u(t_{umax}) - ma(t_4)}{v(t_4)}$$

Assuming the damping constant does not change throughout the event, the value C_4 permits calculation of the static soil resistance F_u for all times t. With the displacement function $u(t)$, a relationship between static soil resistance and displacement may be calculated.

Analysis of the UBC Test Pile Results

The above interpretation approach has been applied to the Statnamic load test data of Piles 3, 4 and 5. Pile 3 is a closed-end pile with its toe at 16.8 m depth, whereas Pile 4 is an opened-end pile with its toe at 23.2 m depth, both pile toes being embedded in the sand deposit underlying the upper silty clay unit. Pile 5 is close-ended and has its toe in the lower clayey silt unit at 31.1 m depth. The Statnamic test data are shown in Fig. 6 to 9, along with results of the static QML tests and the calculated or "predicted" static response derived from the Statnamic test data as described above.

The issue of depicting data derived from the reloading of piles is demonstrated using the results of testing on Pile 3. Figure 6 shows the load-displacement information derived from the Statnamic load test as a reloading event, i.e. with the zero deflection point offset by the displacement of the initial static QML result. The plot suggests that the Statnamic-predicted static load-deflection curve is indicative of reloading a pile. It exhibits the strain hardening or residual stress condition of a pile with a strain history. This would be the preferred method of plotting load test results derived from a reloaded pile. However, uncertainty on the pile rebound after the original static load test was conducted and the effects of restriking the piles confused the issue of how best to depict the data in this study. As a comparison, Fig. 7 shows the same data for Pile 3, but with the results plotted from the same zero point or origin. This plot permits a comparison of the Statnamic-derived pile stiffness through the elastic region of loading with the static load test results.

During the Statnamic load testing of Pile 3, the displacement time history was prematurely cutoff when the laser sensor moved past the laser signal. The loss of the Statnamic return signal inhibits the application of the Statnamic interpretive methodology since the point of maximum deflection (which was lost) is needed in the calculation of system damping. The prediction displayed in Figs. 6 and 7 is made by using the equivalent damping constant (47 MN/s/m^3)

derived from the analysis of Pile 4. The shape of the static prediction curve is arrived through the use of a best fit hyperbolic curve through the estimated point of maximum static deflection. The results demonstrate the accuracy of the method in predicting pile stiffness within the elastic range of response. The failure load as calculated using Davisson's method on the Statnamic-derived static load simulation is 690 kN, compared to 610 kN from the static QML curve.

Figure 8 shows the results of the tests performed on Pile 4, an open-ended pile. The figure displays a typical Statnamic load trace for a pile loaded beyond its ultimate dynamic capacity. The curve exhibits a rounding at the peak load with a deep hysteretic loop on unloading and permanent deflection at the end of the test. These characteristics are important in ensuring that the trace will provide a good prediction of ultimate static capacity. The Statnamic-derived static response indicates a higher estimate of failure load, i.e. 1500 kN, compared to 1200 kN as suggested by the static load test. However, it should be noted that the static load-deflection curve shown, as reported by Robertson et al. (1988), was extrapolated beyond 700 kN based on the results of testing on the other piles. This extrapolation clearly introduces a significant uncertainty for comparing the results of the static and Statnamic load tests for Pile 4.

Figure 9 shows results of the tests performed on Pile 5. The Statnamic curve shows a highly elastic response with little hysteresis and little to no permanent deflection. This indicates that the pile has not been loaded beyond its ultimate dynamic capacity, even though the pile was loaded well beyond the static capacity. The contribution of inertia and damping to the response of the pile-soil system is high. Several factors contribute to the behaviour exhibited. The weak saturated soils, including the clayey silt at the pile toe, are highly viscoelastic. Dynamic loading results in an apparent increase in peak soil resistance. Pile 5 also has a high length to diameter (l/d) ratio, which when combined with its low end bearing resistance creates a very flexible pile-soil system. Thus a large load and correspondingly large displacement are required to fully mobilize the pile. The Statnamic method requires full mobilization of the pile and soil such that a 'release' of the pile from the soil occurs. It is the reattachment of the soil onto the pile at the peak displacement point (zero velocity) that assists in defining the failure damping constant and in determining the peak static load resistance. The damping factor obtained for Pile 4 is used for the estimate made for Pile 5 in Fig. 9 and proves to be too low. This is not surprising since the piles are of different lengths and penetrate to bearing in different soil strata.

CONCLUSIONS

Statnamic load testing experiences to date have shown that the test method can provide reliable estimates of static pile stiffness and ultimate pile capacity in non cohesive and stiff cohesive soils. The Statnamic results, however, are more difficult to interpret for long piles embedded in saturated soft fine-grained soils with high viscoelastic or damping properties. The present study shows that the recent method of interpretation of the Statnamic load test can provide good results for prediction of static pile-load deflection in highly viscoelastic soils provided certain conditions are met. The pile must be fully mobilized by the Statnamic loading to provide a point of static equilibrium prior to unloading of the pile. This permits calculation of system damping and a reasonable estimate of ultimate static pile capacity. The results from this study are

encouraging, but more Statnamic testing is recommended to enhance the current data base and to improve the interpretive procedures.

REFERENCES

Bermingham, P. and Janes, M. 1989. An innovative approach to load testing of high capacity piles. Proc. Int. Conf. on Piling and Deep Foundations, London, 1: 409-413.

Middendorp, P. 1993. First experiences with Statnamic load testing of foundation piles in Europe. 2nd Int. Geotech. Seminar on Deep Foundations on Bored and Auger Piles, Ghent University, Belgium.

Middendorp, P., Bermingham, P., and Kuiper, B. 1992. Statnamic load testing of foundation piles. Proc. of the 4th Int. Conf. on the Application of Stress-Wave Theory to Piles, The Hague, The Netherlands, A.A. Balkema Publishers, 581-588.

Rausche, F., Goble, G.G., and Likins, G. 1985. Dynamic determination of pile capacity. Journal of Geotech. Engin., ASCE, 111(3): 367-387.

Robertson, P.K., Campanella, R.G., Davies, M.P., and Sy, A. 1988. Axial capacity of driven piles in deltaic soils using CPT. Penetration Testing 1988, Proc. ISOPT-1, A.A. Balkema Publishers, 2: 919-928.

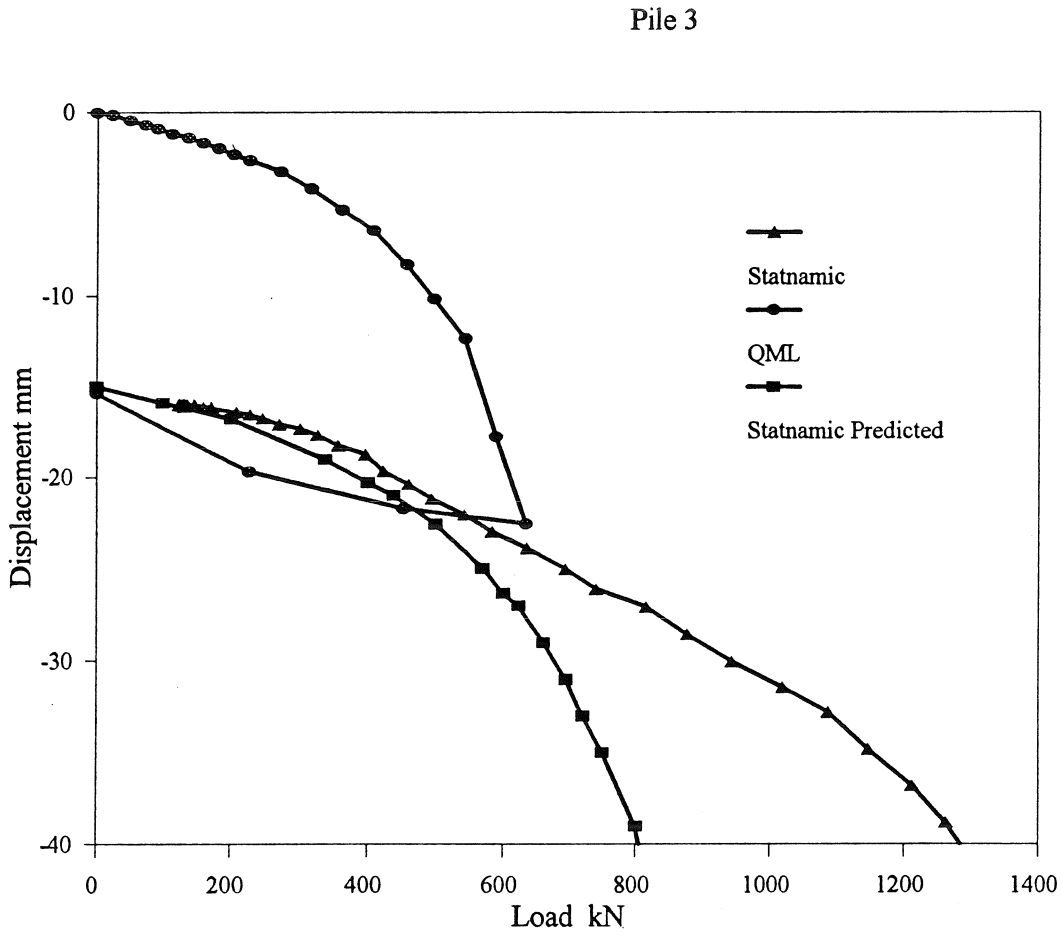

Fig. 6 Statnamic and static load test results for Pile 3 with displacement offset

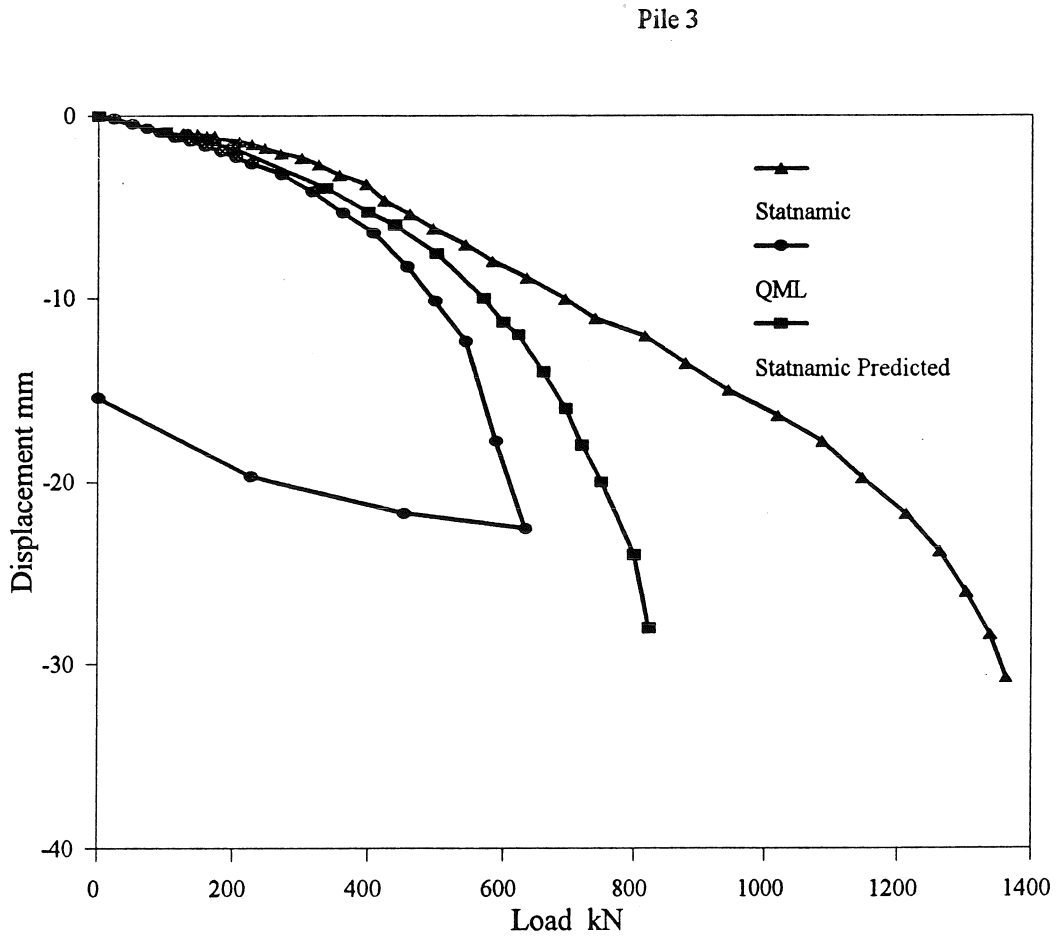

Fig. 7 Statnamic and static load test results for Pile 3
no displacement offset

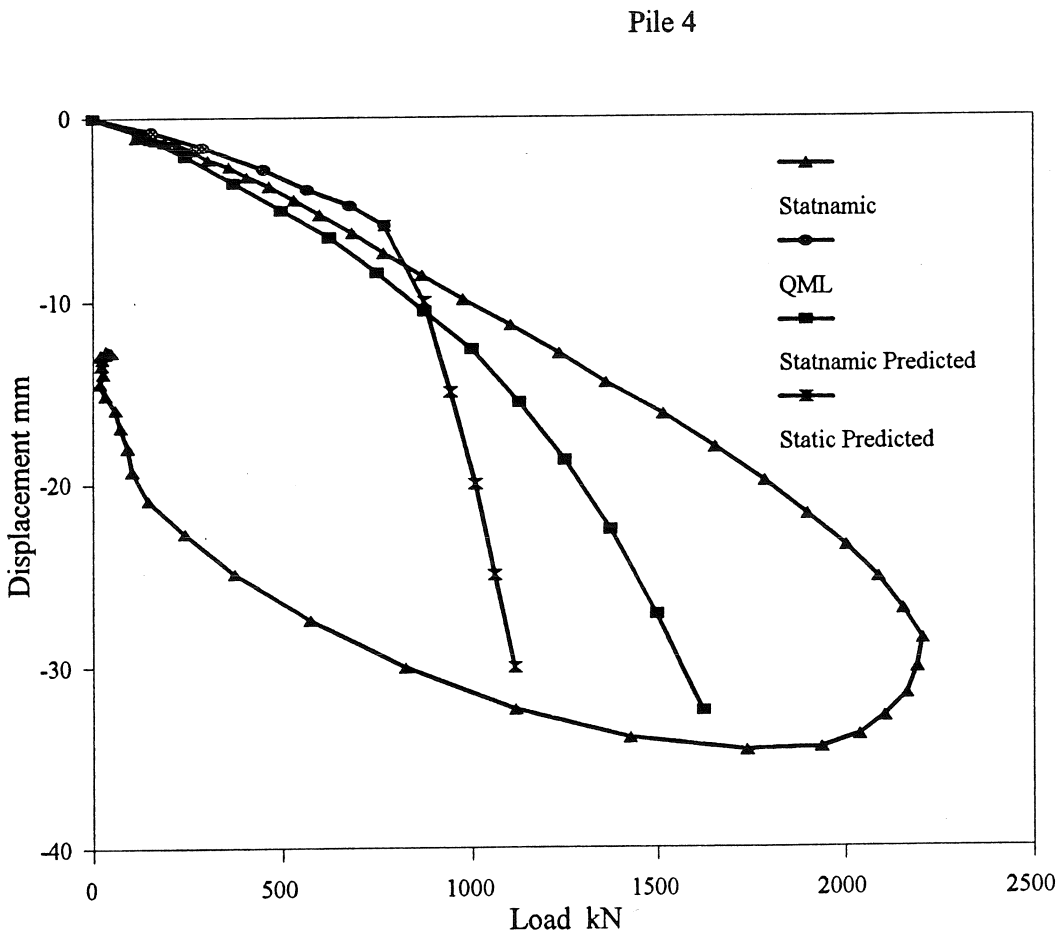

Fig. 8 Statnamic and static load test results for Pile 4

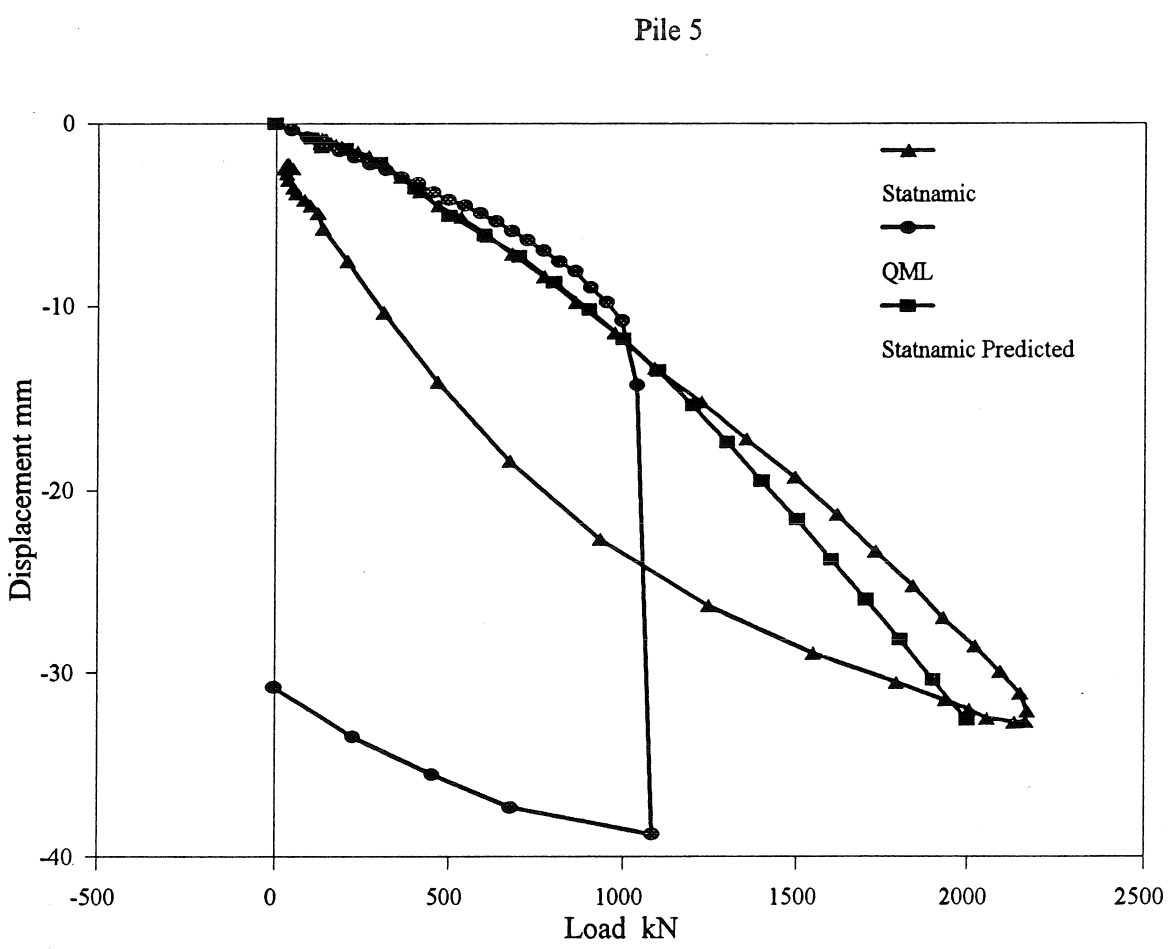

Fig. 9 Statnamic and static load test results for Pile 5